Table S1. Characterization of the studied MOFs and their composites.

MOF or MOF-Composite	Langmuir Surface Area (m^2/g)	Crystalline lattice parameters (Å)	V (Å^3)
CuBTC	-	a, b, c = 26.3152(6)	18223.14(9)
CuBTC-A-15	1716.48	a, b, c = 26.3302(1)	18254.19(9)
CuBTC-Mt-15	-	a, b, c = 26.3341(5)	18262.42(2)
CuBTC-BC-5	1502.17	a, b, c = 26.3485(6)	18292.40(9)
CuBTC-BC-15	620.32	a, b, c = 26.3131(1)	18218.65(9)
CuBTC-BC-30	-	a, b, c = 26.3084(1)	18208.91(1)
UTSA-16	-	a, b = 13.0075(3), c = 30.1528(6)	5101.74(6)
UTSA-16-Mt-5	676.23	a, b = 13.0562(3), c = 30.0278(2)	5118.69(8)
UTSA-16-Mt-15	-	a, b = 12.9900(6), c = 30.1602(8)	5089.29(8)
UTSA-16-Mt-40	-	a, b = 13.0005(5), c = 30.1834(7)	5101.44(6)
UiO-66-BTEC	-	a, b, c = 20.6969(2)	8865.79(4)
UiO-66-BTEC-A-15	330.31	a, b, c = 20.7930(8)	8989.94(1)
UiO-66-BTEC-Mt-15	543.40	a, b, c = 20.6568(8)	8814.43(9)
UiO-66-BTEC-BC-5	-	a, b, c = 20.7165(5)	8891.03(9)
UiO-66-BTEC-BC-15	567.76	a, b, c = 20.6858(8)	8851.61(1)
UiO-66-BTEC-BC-30	-	a, b, c = 20.7279(1)	8905.66(2)

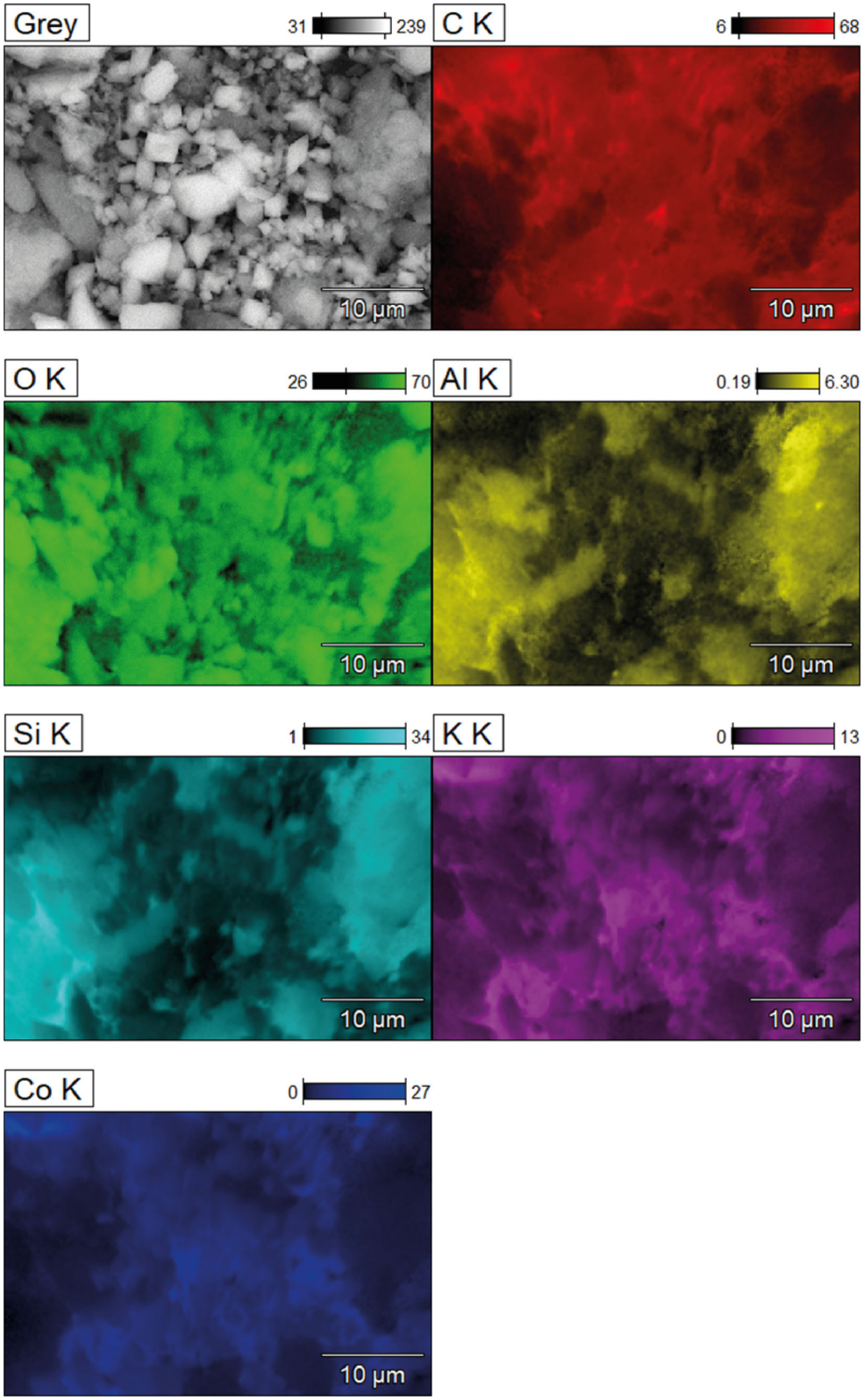

Figure S1: EDS element mapping image of UTSA-16-Mt-15

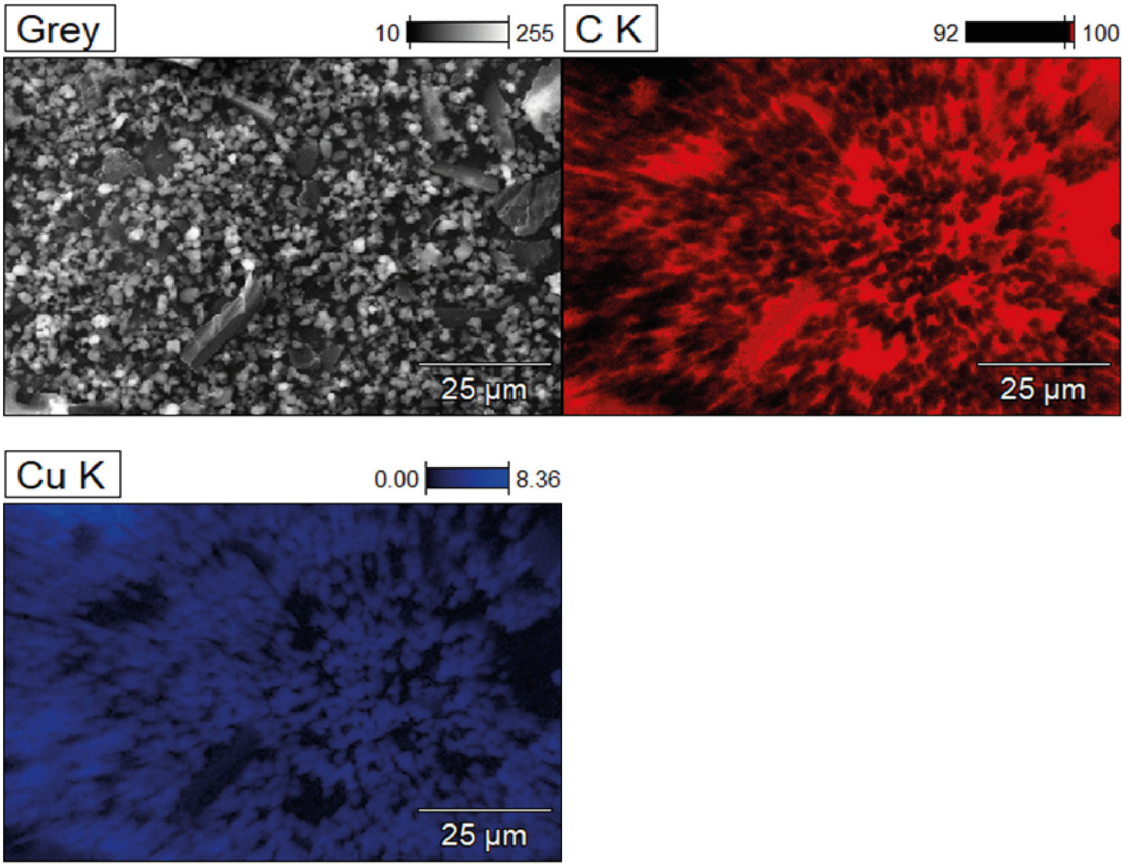

Figure S2. EDS element mapping image of CuBTC-BC-15.

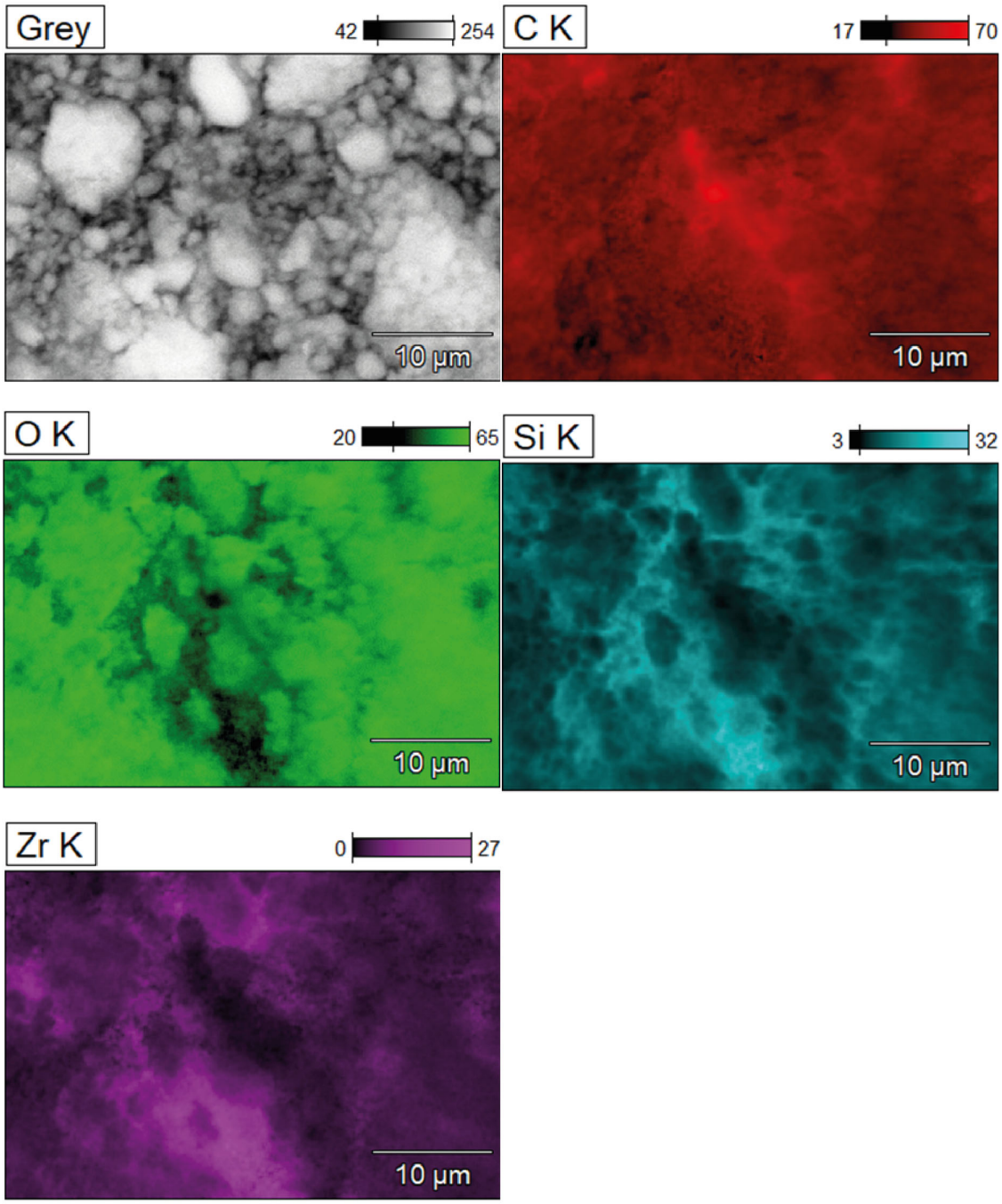

Figure S3. EDS element mapping image of UiO-66-BTEC-A-15.

Table S2. Content of the elements in MOFs and their composites.

MOF or MOF-Composite	C (%)	Si (%)	Al (%)	Cu (%)	Co (%)	K (%)	Zr (%)
CuBTC	43±3	0.019±0.007	-	25.5±0.1	-	0.22±0.02	-
CuBTC-A-15	28.4±0.9	0.039±0.004	-	27.7±0.5	-	-	-
CuBTC-Mt-15	20.5±0.1	0.033±0.004	2.36±0.09	12.0±0.9	-	0.25±0.04	-
CuBTC-BC-5	39.2±0.7	0.039±0.008	-	25.8±0.2	-	0.16±0.04	-
CuBTC-BC-15	42±5	0.0341±0.0004	0.020±0.003	20.9±0.2	-	0.36±0.01	-
CuBTC-BC-30	45±1	0.049±0.002	0.026±0.002	19.3±0.1	-	0.24±0.03	-
UTSA-16	19.0±0.4	-	-	-	22.2±0.2	9.60±0.08	-
UTSA-16-Mt-5	16.2±0.1	0.079±0.005	0.35±0.03	-	18.73±0.01	10.532±0.004	-
UTSA-16-Mt-15	15±1	0.070±0.01	1.0±0.5	-	14.9±0.9	8.2±0.4	-
UTSA-16-Mt-40	12.9±0.8	0.058±0.004	2.34±0.06	-	10.7±0.3	8.35±0.03	-
UTSA-16-A-15	14±2	0.032±0.004	-	-	12±1	9.22±0.03	-
UTSA-16-BC-15	29.8±0.3	0.08±0.02	0.019±0.002	-	17.1±0.6	8.6±0.2	-
UiO-66-BTEC	19.8±0.9	-	-	-	-	-	20.1±0.3
UiO-66-BTEC-A-15	21.6±0.3	0.053±0.005	-	-	-	-	18.09±0.07
UiO-66-BTEC-Mt-15	21.3±0.3	0.065±0.004	0.31±0.04	-	-	0.16±0.08	18.9±1
UiO-66-BTEC-BC-5	29.7±0.5	0.058±0.007	-	-	-	-	19.5±0.3
UiO-66-BTEC-BC-15	33.4±0.3	0.039±0.002	-	-	-	0.185±0.004	17.5±0.4
UiO-66-BTEC-BC-30	39.1±0.9	0.091±0.002	-	-	-	0.14±0.03	14.59±0.07

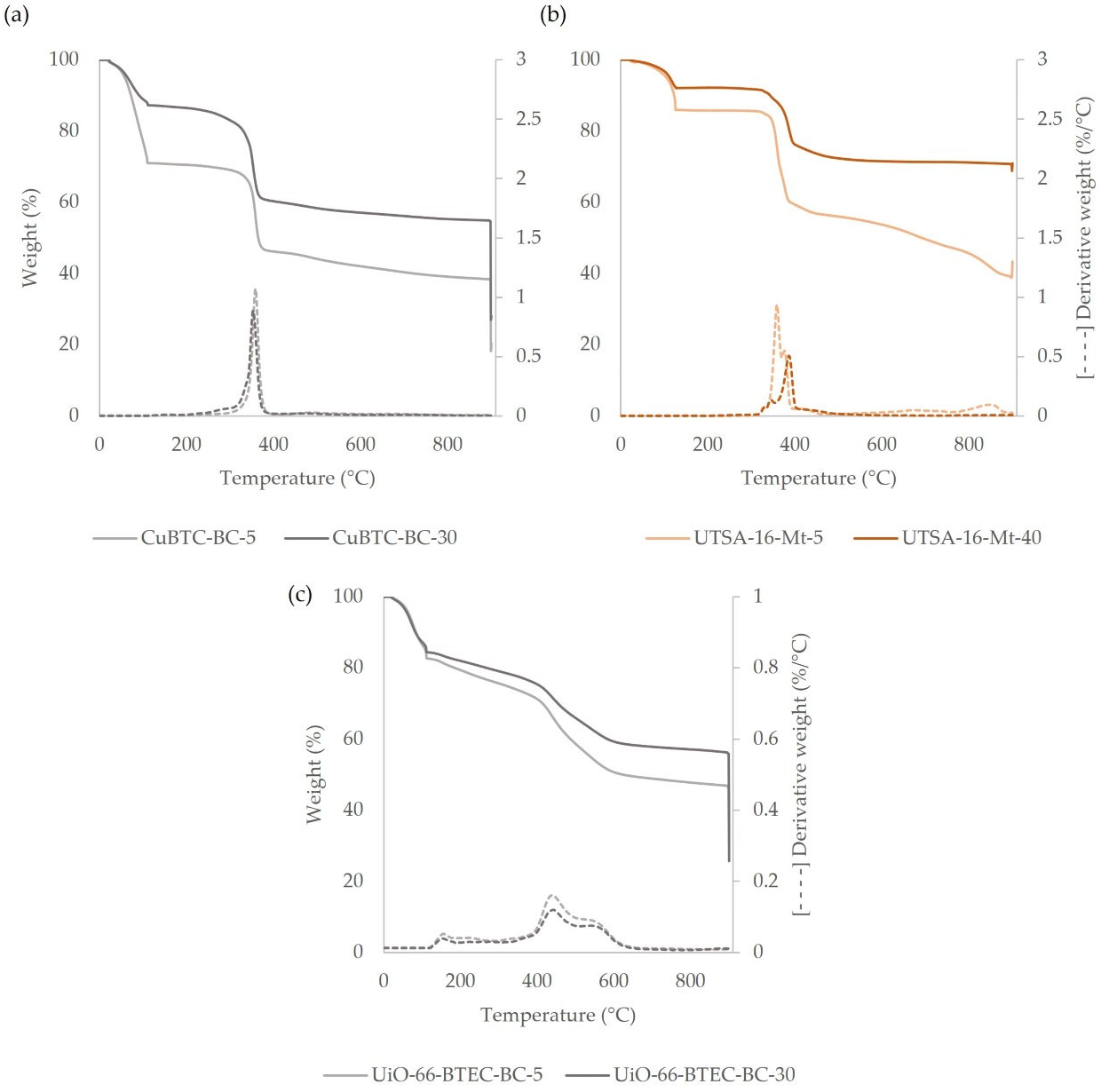

Figure S4: Thermogravimetric analysis (TGA) of MOF-composites: a) CuBTC-composites; b) UTSA-16-composites; c) UiO-66-BTEC-composites.

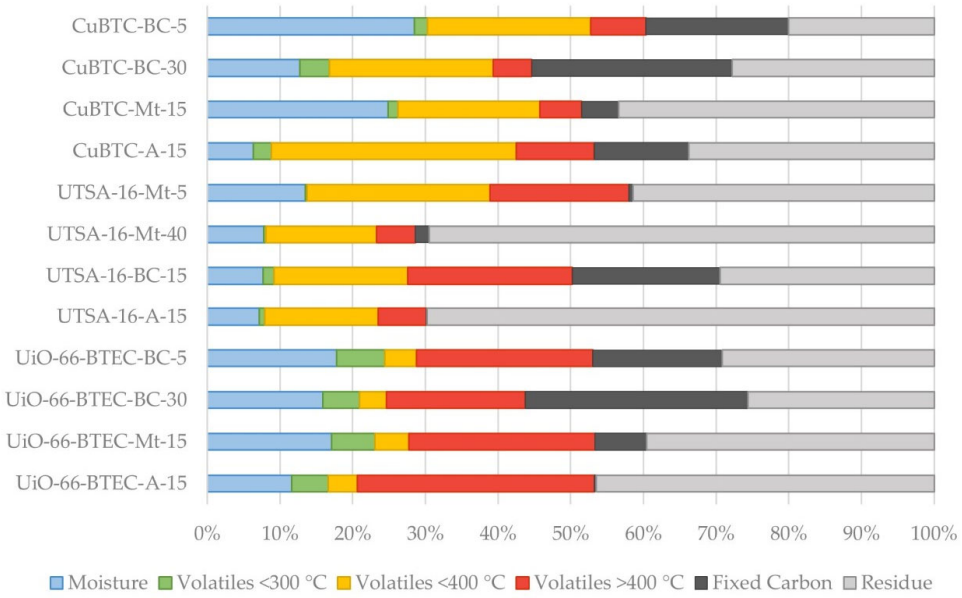

Figure S5. Thermal degradation matrix of MOF-composites.

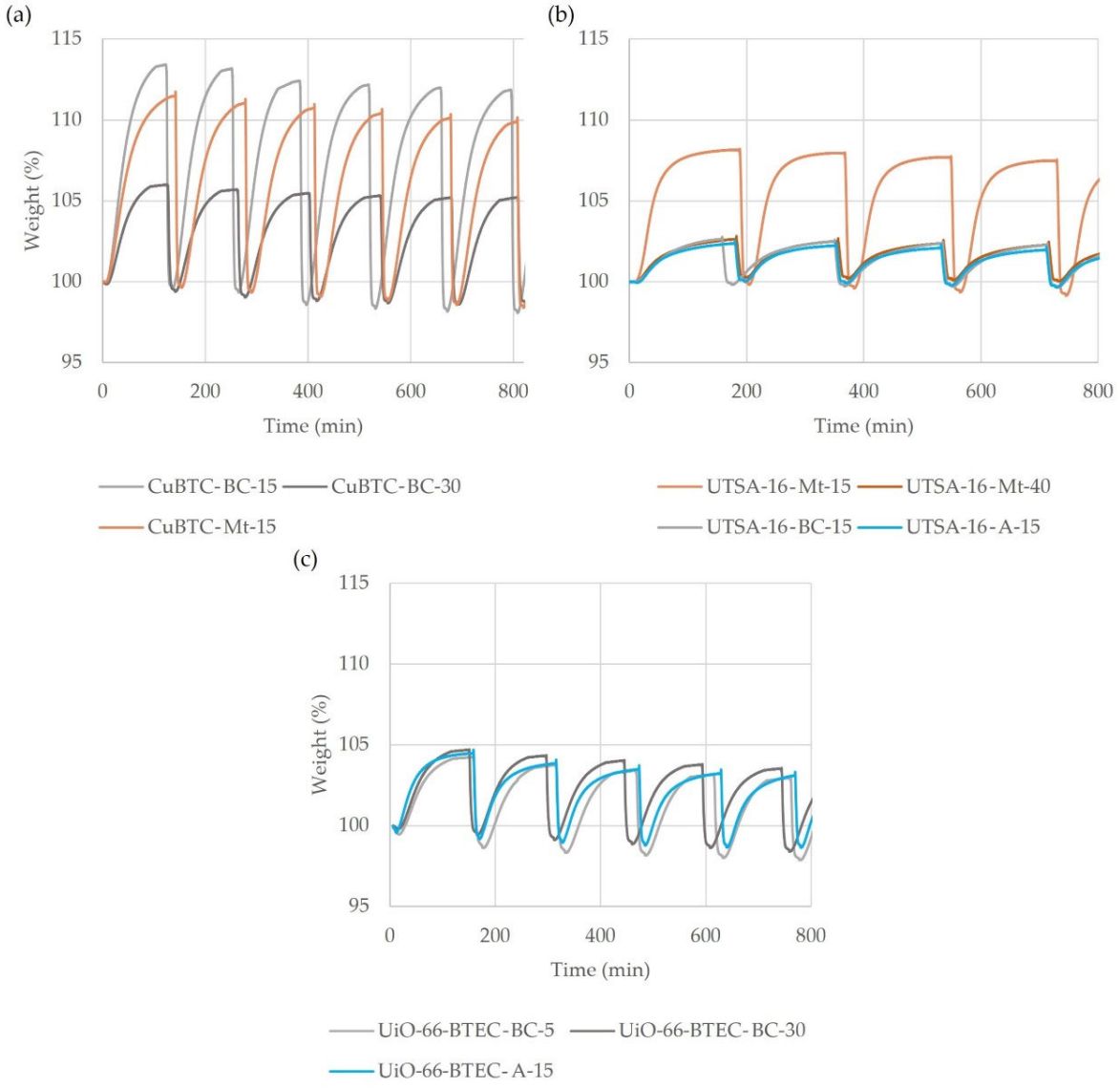

Figure S6. CO_2 sorption and desorption cycles of MOF-composites: a) CuBTC-composites; b) UTSA-16-composites; c) UiO-66-BTEC-composites.

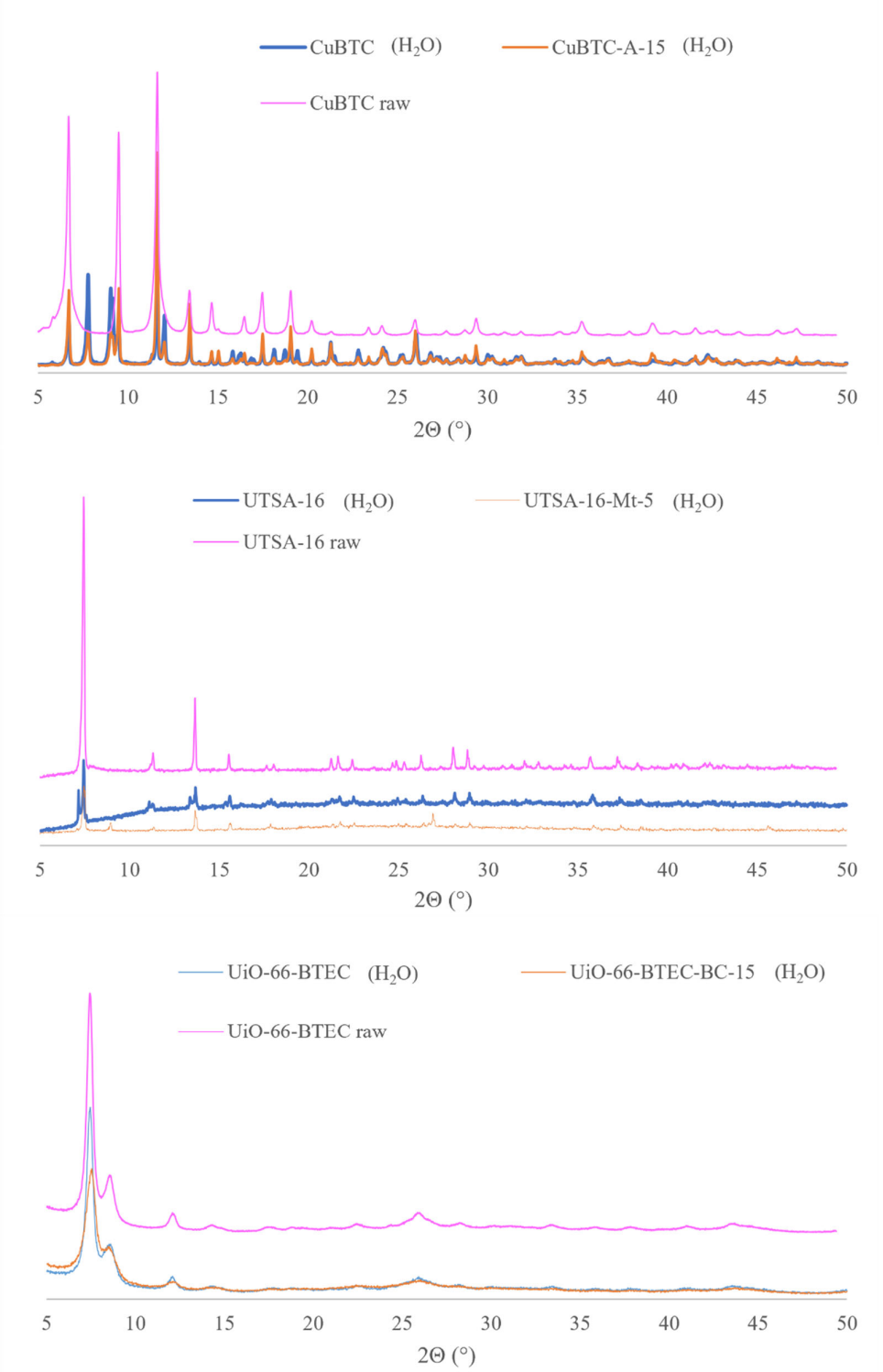

Figure S7. PXRD spectra of CuBTC (H_2O) after exposure to water, raw CuBTC and CuBTC-composite containing aerosil (CuBTC-A-15 (H_2O)) after exposure to water. PXRD spectra of UTSA-16 (H_2O) after exposure to water, raw UTSA-16 and UTSA-16-composite containing montmorilonite (UTSA-16-Mt-5 (H_2O)) after exposure to water. PXRD spectra of UiO-66-BTEC (H_2O) after exposure to water, raw UiO-66-BTEC and UiO-66-BTEC-composite containing biochar (CuBTC-BC-15 (H_2O)) after exposure to water.